Retinal dysfunction characterizes subtypes of dominant optic atrophy

Maria Lucia Cascavilla,[1] Vincenzo Parisi,[2] Giacinto Triolo,[1] Lucia Ziccardi,[2] Enrico Borrelli,[1] Antonio Di Renzo,[2] Nicole Balducci,[3] (iD) Costanza Lamperti,[4] Stefania Bianchi Marzoli,[5] Fatima Darvizeh,[1] Alfredo A. Sadun,[6] Valerio Carelli,[7,8] Francesco Bandello[1] and Piero Barboni[1]

[1]Scientific Institute San Raffaele Via Olgettina, Milan, Italy
[2]"G.B. Bietti" Foundation - IRCCS, Rome, Italy
[3]Studio Oculistico d'Azeglio, Bologna, Italy
[4]Unit of Molecular Neurogenetics, Foundation "C. Besta" Neurological Institute-IRCCS, Milan, Italy
[5]Neuro-ophthalmology Unit, Department of Ophthalmology, IRCCS Istituto Auxologico Italiano, Milano, Italy
[6]Department of Ophthalmology, Dohene Eye Institute, UCLA, Pasadena, CA, USA
[7]IRCCS, Istituto delle Scienze Neurologiche di Bologna, Bologna, Italy
[8]Neurology Unit, Department of Biomedical and Neuromotor Sciences (DIBINEM), University of Bologna, Bologna, Italy
[Correction added on 25 October 2017, after first online publication: Author affiliations (7) and (8) have been corrected in this current version.]

ABSTRACT.

Purpose: To assess preganglionic retinal function using multifocal electroretinogram (mfERG) in patients affected by dominant optic atrophy (DOA) stratified by *OPA1* gene mutation.

Methods: Multifocal electroretinogram (mfERG) was recorded in 18 DOA patients (DOA group, 35 eyes) and 25 age-matched healthy subjects (control group, 25 eyes). Patients were stratified in two groups based on gene mutation: missense mutation (DOA-M group, 11 eyes) and mutation causing haploinsufficiency (DOA-H group, 24 eyes). The mfERG N1-P1 response amplitude density (RAD) has been evaluated in five annular retinal areas with different eccentricity from the fovea (ring 1: 0–5 degrees, R1; ring 2: 5–10 degrees, R2; ring 3: 10–15 degrees, R3; ring 4: 15–20 degrees, R4; and ring 5: 20–25 degrees, R5) and in eight sectors on the basis of the retinal topography: temporal–superior (TS), temporal–inferior (TI), nasal–superior (NS) and nasal–inferior (NI), temporal (T), superior (S), nasal (N) and inferior (I).

Results: Compared to controls, DOA group revealed a significant reduction in N1-P1 RADs values in R1-R4 rings and in TI, NS and N sectors [analysis of variance (ANOVA), p < 0.01]. DOA-M group showed a significant reduction in N1-P1 RADs values in R1-R5 rings and in TI, NS, NI, T, N and I sectors (p < 0.01). Dominant optic atrophy-H (DOA-H) group displayed only a significant (p < 0.01) reduction in N1-P1 RADs values, exclusively in R1 and in the NS sector.

Conclusion: Preganglionic retinal impairment occurs in DOA with a clear genotype to retinal dysfunction association. Missense mutations are characterized by a far more severe functional impairment.

Key words: dominant optic atrophy – multifocal electroretinogram – *OPA1* gene – photoreceptors – retinal topography

Introduction

Dominant optic atrophy (DOA) is a neurodegenerative disorder with an early age of onset characterized by central vision loss due to retinal ganglion cell (RGC) degeneration, ultimately resulting in severe optic atrophy (Lenaers et al. 2012). The disease has incomplete penetrance and variable expression, between and within families, which ranges from subclinical manifestations to legal blindness. The most commonly affected gene is *OPA1*, located on the long arm of chromosome 3 (3q28–q29), (Alexander et al. 2000; Delettre et al. 2000), and more than 300 different mutations have been described (http://mitodyn.org, last update April 22, 2016). Disease hallmarks include bilateral and progressive visual loss, central visual field (VF) defects, colour discrimination disturbances and optic disc pallor.

An emerging genotype/phenotype correlation highlights the difference in severity between *OPA1* mutations leading to haploinsufficiency (DOA-H) and *OPA1* missense mutations (DOA-M), for which a dominant negative effect has been proposed (Yu-Wai-Man et al. 2011). Moreover, a genotype–phenotype correlation has been established by analysing macular ganglion cells

(GC-IPL) thickness: DOA-M patients had thinner GC-IPL than DOA-H (Barboni et al. 2014).

A dysfunction of the innermost retinal layers (RGCs and their fibres) has been described in DOA patients, as suggested by abnormal pattern electroretinogram (PERG) responses (Holder et al. 1998-1999; Morny et al. 2015). A few reports described preganglion retinal elements in DOA, but the data have been discordant between humans (Miyata et al. 2007; Reis et al. 2013) and animal models (Heiduschka et al. 2010; Barnard et al. 2011).

The mfERG technique is useful to assess the bioelectrical responses derived from different retinal areas (Hood et al. 2003; Barnard et al. 2011). A 'kernel' analysis applied to mfERG responses can be used to assess nonlinear functions of the visual system (Bearse & Sutter 1996), and it was recognized that the first-order kernel of mfERG originates in the preganglionic elements (photoreceptors and bipolar cells) (Hood 2000). The 'kernel analysis' was particularly useful to assess that in glaucoma, a not exclusive dysfunction of the GCs and their fibres (mainly detected by PERG recordings, see Wilsey & Fortune 2016 as a review) was present, but that a functional impairment of the preganglionic elements may also occurs (Chan & Brown 2000; Chan 2005; Chan et al. 2011; Parisi et al. 2012).

Therefore, our aim is to evaluate, by mfERG recordings, the function of preganglionic elements in DOA patients. In addition, our work points out to assess whether the possible dysfunction can be detectable in the macular region and/or in the more peripheral retinal areas, or in selected retinal sectors. Moreover, we evaluated the association between DOA genotypes and the possible detectable preganglionic dysfunction by stratifying DOA patients in those with OPA1 missense mutations and those with OPA1 mutations causing haploinsufficiency.

Patients and Methods

Patients

Eighteen DOA patients (mean age: 42.0 ± 16.3 years, range: 10–76 years) from 14 unrelated pedigrees with a molecularly confirmed diagnosis of OPA1 mutation were evaluated at the University Eye Clinic of San Raffaele Hospital between 2010 and 2013 and enclosed in this study.

On the basis of specific OPA1 mutations, DOA patients were divided into two groups: OPA1 missense mutation (DOA-M Group) and OPA1 mutations causing haploinsufficiency (DOA-H Group).

A group of 25 age-matched healthy subjects (mean age: 38.8 ± 13.3 years, range: 16–64 years, 25 eyes) evaluated during a routine ophthalmological examination served as controls.

All participants gave their informed consent according to the Declaration of Helsinki, and the study was approved by the Internal Review Board at the University Eye Clinic of San Raffaele Hospital, Milan.

All subjects had an extensive ophthalmologic examination, including best corrected visual acuity (BCVA) expressed as the logarithm of the minimum angle of resolution (logMAR) and Humphrey VF examination (SITA 24-2 standard test, HFA II 750-4.1 2005, Carl Zeiss Meditec Inc, USA).

Control subjects had an intraocular pressure (IOP) lower than 21 mm Hg, BCVA of at least 0.0 logMAR with a refractive error between -2.00 and $+2.00$ spherical equivalent; normal 24-2 VF with mean deviation (MD) $\pm$ 0.5 dB, corrected pattern standard deviation (CPSD) <1 dB, false-positive rate and false-negative rate each <20% and no ocular, metabolic or neurological diseases.

Inclusion criteria for DOA patients were as follows:
(1) No evidence or previous history of glaucoma (IOP lower than 21 mmHg) or any other optic neuropathy other than DOA;
(2) 24-2 HFA VF with MD between -2 and -12 dB, CPSD between $+2$ and $+10$ dB, false-positive rate and false-negative rate each $< 20\%$;
(3) Ability to maintain a stable fixation comparable to that of normal subjects (fixation loss rate ranging between 4% and 6%);
(4) Corrected BCVA ranging from 0.0 to 0.8 logMAR;
(5) One or more papillary signs of DOA: the presence of a localized or total loss of neuroretinal rim, thinning of the neuroretinal rim, generalized loss of optic rim tissue, optic nerve pallor;
(6) Refractive error (when present) between -2.00 and $+2.00$ spherical equivalent;

(7) No previous history or presence of any ocular disease involving cornea and lens and ocular surgery, which could interfere with data interpretation;
(8) No previous history or presence of early signs of maculopathy or retinal diseases and metamorphopsia recording of the Amsler test. The macular clinical evaluation was based on slit-lamp and indirect ophthalmoscopic examination using $+90-+78$ D no-contact lens (Volk Optical, Mentor, OH, USA) after pupillary dilatation using tropicamide 1%;
(9) No previous history or presence of detectable spontaneous eye movements (i.e. nystagmus);
(10) No previous history or presence of diabetes, optic neuritis, any disease involving the visual pathways, or drug intake that can interfere with macular function; and
(11) Pupil diameter < 3 mm without mydriatic or miotic drugs.

Excluded from this study were also all eyes with a 24-2 Humphrey VF showing a centrocecal scotoma that did not allow perceiving the target of the multifocal mfERG stimulation and with no good target fixation.

MfERG recordings

Multifocal ERG was measured by RETIMAX (CSO, Florence, Italy) using a standardized method (Hood et al. 2012).

The multifocal stimulus, consisting of 61 scaled hexagons, was displayed on a high-resolution, black-and-white monitor (size 30 cm, width and 30 cm height) with a frame rate of 75 Hz. The array of hexagons subtended 25 degrees of VF. Each hexagon was independently alternated between black (1 cd/m^2) and white (200 cd/m^2) according to a binary m-sequence. This resulted in a contrast of 99%. The luminance of the monitor screen and the central fixation cross (used as target) was 100 cd/m^2. The m-sequence had $2^{13}-1$ elements, and total recording time was approximately 4 min. Total recording time was divided into eight segments. Between segments, the subject was allowed to rest for a few seconds. Focusing lenses were used when necessary. To maintain a stable fixation, a small red target (0.5 deg) was placed in the centre of the stimulation field. At every mfERG

examination, each patient positively reported that he/she could clearly perceive the cross fixation target. The eye's position was continuously monitored by an external video system to track fixation losses.

Multifocal electroretinograms (mfERGs) were monocularly recorded in the presence of pupils that were maximally pharmacologically dilated with 1% tropicamide to a diameter of 7–8 mm. Pupil diameter was measured by an observer (MLC) by means of a millimeter ruler and a magnifying lens and stored for each tested eye. The cornea was anaesthetized with 1% lidocaine. Multifocal electroretinograms (mfERGs) were recorded bipolarly between an active Dawson–Trick–Litzkow (DTL) bipolar contact electrode and a reference electrode (Ag/AgCl electrode placed on the correspondent temporal side of the frontal lobe). A small Ag/AgCl skin ground electrode was placed at the centre of the forehead. Interelectrode resistance was <3 KOhms.

The signal was amplified (gain 100.000) and filtered (band-pass 1–100 Hz). After automatic rejection of artefacts, the first-order kernel response was examined. For each obtained averaged response, we evaluated the RAD between the first negative peak, N1, and the first positive peak, P1 (N1-P1 RAD, expressed in $nV/degree^2$).

We considered three possible retinal topographies to explore the bioelectrical responses derived from specific retinal areas. Data analysed were as follows:

1 Ring analysis: the averaged response obtained from five concentric annular retinal regions (rings) centred on the fovea: from 0 to 5 degrees (ring 1, R1), from 5 to 10 degrees (ring 2, R2), from 10 to 15 degrees (ring 3, R3), from 15 to 20 degrees (ring 4, R4) and from 20 to 25 degrees (ring 5, R5).

2 Sector analysis 1: the averaged response obtained from quadrants analysis centred on the vertical and the horizontal meridians compliant with the topography of the retinal nerve fibre layers (RNFL): NI, NS, TI and TS sectors. As the main mfERG response is recorded in the central retina (see 'Ring analysis'), the bioelectrical responses obtained from the more central retina stimulation (0–5 degrees) have been excluded from this analysis.

3 Sector analysis 2: the averaged response obtained from quadrants analysis centred on the 25 degrees from the horizontal and vertical meridians compliant with the topography of the RNFL: N, S, I and T sectors. The bioelectrical responses obtained from the more central retina stimulation (0–5 degrees) have been excluded also in this case.

Signal-to-noise ratio

Multifocal electroretinogram (mfERG) signal-to-noise ratio (SNR) was estimated following the methodology discussed in previously published studies (Parisi et al. 2010, 2012). Briefly, a noise window was set as that part of the record that was of equal length to the period within which the response was analysed, but it was included in a temporal window that was assumed to contain little or no response. Signal temporal window for the mfERG was 0–80 ms, while the noise temporal window was 80–160 ms. Signal-to-noise ratio was defined as the ratio of root mean square (RMS) signal plus noise (measured in the signal temporal window) of a given record to the mean RMS of all noise windows (61 for the mfERG). A SNR of ≥3 was accepted for mfERG 'recordable' responses.

Statistics

Electrophysiological data form controls and DOA patients were normally distributed. Data from control and patient groups (whole DOA and separately DOA-M and DOA-H groups) were analysed by the one-way analysis of variance (ANOVA) test. All statistical analyses were performed using MedCalc V.13.0.4.0 (MedCalc, Mariakerke, Belgium), and a p value <0.01 was considered as statistically significant.

Results

Thirty-five eyes of 18 DOA patients from 14 unrelated pedigrees were included in the study. Twelve patients (24 eyes) belonged to DOA-H group (mean age 44.02 ± 16.24 years), and six patients (11 eyes, mean age 37.72 ± 16.27 years as one eye was excluded on the basis of the above established exclusion criteria) belonged to DOA-M group.

Table 1 shows the *OPA1* mutations type in the 14 pedigrees stratified by mutational category. Patients from pedigrees carrying the same mutation were pooled together. Most mutations are well established as pathogenic and listed in the *OPA1* mutation database (http://mitodyn.org, accessed May 2016); other mutations have been more recently reported or are unpublished, still obeying the establshed criteria for pathogenicity.

Table 2 reports the individual mfERG N1-P1 RAD values from five different annular retinal areas with different eccentricity from the fovea and from eight sectors on the basis of the retinal topographies described in Methods.

Considering the lower limit (LL) obtained from control subjects by calculating mean values −2 standard deviations of mfERG N1-P1 RADs for each examined ring and sector, we

Table 1. *OPA1* mutations in dominant optic atrophy (DOA) patients, described according to variant 1, RefSeq: NM_015560.2.

Number of pedigree	Number of affected patients	OPA1 mutations		OPA1 exon/intron	M/H
3	5	*c.2708-2711delTTAG*	*p.Val903Glyfs3*	27	H
1	1	*c.2825-2828delAGTT*	*p.Lys941 fs26*	28	H
1	1	*c.1783insT*	*p.Glu594*	19	H
1	1	*c.2196-2197dupAGAC*	*p.Ser732Profs*	22	H
1	1	*c.2569 C > T*	*p.Arg857*	25	H
1	1	*c.1770 + 1 delG*	*splice defect*	intron 18	H
1	1	*c.870 + 5G > A*	*splice defect*	intron 8	H
1	1	*c.1212 + 1G > A*	*Splice deficit*	intron 12	H
2	4	*c.1409A > G*	*p.Asp470Gly*	14	M
1	1	*c.1334G > A*	*p.Arg445His*	14	M
1	1	*c.2797G > A*	*p.Val933Ilesf*	27	M

H = mutation causing haploinsufficiency, M = missense mutation.

Table 2. Individual multifocal electroretinogram (mfERG) N1-P1 response amplitude density (RAD, nV/degree^2) values recorded in patients affected by dominant optic atrophy with *OPA1* missense mutation (DOA-M) and with *OPA1* mutations causing haploinsufficiency (DOA-H).

DOA eye	RAD R1	RAD R2	RAD R3	RAD R4	RAD R5	RAD TS	RAD TI	RAD NS	RAD NI	RAD T	RAD S	RAD N	RAD I
DOA—M#1	65.23*	47.87	29.9	17.85	18.57	16.01	28.28	18.76	27.62	24.88	15.61	20.05	27.79
DOA—M#2	75.03*	40.78	29.72	11.15*	17.09	9.61*	23.4	16.86	26.17	16.08	11.85	25.51	26.86
DOA—M#3	41.72*	46.88	17.87*	22.01	16.68	21.25	21.19	24.79	14.21*	12.77*	27.92	15.87*	12.64*
DOA—M#4	67.68*	23.67*	18.16*	11.07*	11.15	17.23	11.14*	14.77*	13.34*	12.04*	15.91	14.15*	13.66*
DOA—M#5	53.9*	22.94*	16.32*	10.01*	9.11*	15.55	11.00*	11.18*	13.26*	12.53*	11.17*	9.19*	13.42*
DOA—M#6	94.83*	34.71*	18.17*	10.84*	11.28	19.03	11.71*	19.56	18.41	12.12*	14.95	21.93	12.68*
DOA—M#7	53.87*	27.61*	17.33*	10.22*	8.92*	10.61*	12.06*	14.14*	13.36*	11.31*	11.05*	10.77*	12.96*
DOA—M#8	37.95*	32.12*	17.41*	11.25*	12.24	14.32	13.89*	14.71*	24.19	12.89*	23.03	15.60*	9.89*
DOA—M#9	58.23*	36.11*	28.82	18.32	10.83	26.21	27.29	26.94	14.00*	26.57	24.88	16.05*	11.76*
DOA—M#10	70.88*	30.03*	16.33*	17.43	9.11*	14.0	15.45*	16.52*	14.15*	12.62*	14.98	14.12*	18.03
DOA—M#11	174.90	71.54	44.0	23.89	18.9	30.44	22.05	31.03	26.83	29.98	27.23	29.94	22.07
DOA—H#1	154.27	79.46	31.9	23.25	19.3	22.54	28.87	21.92	28.54	24.82	21.46	24.32	31.22
DOA—H#2	132.28	55.64	22.96	17.58	13.8	14.81	19.72	19.64	22.88	18.71	16.51	14.12	22.42
DOA—H#3	189.01	96.92	47.58	24.04	25.91	30.36	33.67	30.85	35.89	33.24	27.72	35.72	33.97
DOA—H#4	179.33	88.54	48.03	21.64	21.31	26.51	30.82	21.72	29.41	28.43	21.93	31.9	29.74
DOA—H#5	139.75	70.51	49.15	29.69	24.72	34.28	35.41	26.05	35.16	39.61	25.37	30.34	39.62
DOA—H#6	94.34*	55.83	35.26	22.94	15.91	24.93	26.35	20.18	23.68	30.41	18.52	25.41	22.93
DOA—H#7	63.96*	41.11	25.11	14.69	13.86	17.59	16.71	17.37	20.09	14.34	16.62	18.53	20.89
DOA—H#8	90.45*	47.75	24.77	12.85	11.91	15.49	19.50	20.74	19.53	15.73	15.78	19.79	19.04
DOA—H#9	92.05*	58.19	30.94	12.88	10.73*	18.44	20.19	13.55*	21.88	22.35	14.52	18.52	21.82
DOA—H#10	130.86	81.34	36.44	13.36	14.19	15.93	21.01	26.62	26.85	21.12	19.54	31.34	20.48
DOA—H#11	83.01*	48.29	31.72	24.89	23.58	27.96	31.82	21.54	29.69	37.56	17.02	15.56*	35.57
DOA—H#12	144.62	46.18	33.62	28.24	22.09	18.49	24.59	30.43	28.23	18.06	21.68	29.37	23.78
DOA—H#13	88.62*	40.64	18.27*	16.68	16.14	14.30	27.73	13.64*	12.60*	23.75	13.94	11.12*	24.24
DOA—H#14	92.56*	21.44*	27.63	17.01	16.85	18.73	17.50	13.82	23.14	18.59	12.74	20.23	22.21
DOA—H#15	78.60*	68.69	26.70	19.9	16.11	18.34	22.77	21.99	15.43	23.07	22.86	18.67	22.56
DOA—H#16	164.37	76.21	37.16	19.08	16.83	20.94	26.41	21.89	27.87	25.32	18.68	25.51	28.99
DOA—H#17	66.91*	42.92	23.3	20.43	13.35	22.39	24.94	17.21	20.85	33.32	12.51	16.62	17.72
DOA—H#18	82.92*	33.99*	21.73	18.87	11.91	14.07	18.56	21.92	24.48	14.26	15.66	24.74	24.0
DOA—H#19	203.14	50.70	32.4	15.05	11.42	34.40	27.45	14.55*	27.71	43.42	21.39	20.15	23.87
DOA—H#20	204.97	67.49	25.92	12.28	20.46	28.65	32.05	16.15*	24.11	35.52	21.01	19.58	31.37
DOA—H#21	67.53*	41.46	19.67	13.23	12.74	21.59	14.22*	13.87*	12.01*	18.32	18.91	17.82	12.96*
DOA—H#22	68.87*	39.85	20.50	13.09	11.18	14.44	14.22*	16.45*	14.61	15.41	14.93	15.94*	11.35*
DOA—H#23	111.95	53.49	29.62	17.13	14.61	18.55	20.62	23.85	18.72	18.51	20.39	22.47	19.32
DOA—H#24	108.13	42.05	37.53	18.49	16.85	23.94	21.09	17.79	23.93	27.66	18.47	25.73	20.52
LL	95.65	36.60	18.97	11.75	10.82	10.84	16.23	16.59	14.58	13.11	11.33	16.51	13.70

The mfERG responses have been evaluated in five annular retinal areas with different eccentricity from the fovea (ring 1: 0–5 degrees, R1; ring 2: 5–10 degrees, R2; ring 3: 10–15 degrees, R3; ring 4: 15–20 degrees, R4; and ring 5: 20–25 degrees, R5) and in eight sectors on the basis of the retinal topography: temporal–superior (TS), temporal–inferior (TI), nasal–superior (NS) and nasal–inferior (NI), temporal (T), superior (S), nasal (N) and inferior (I).

LL = lower limit obtained from control subjects by calculating mean values −2 standard deviations.

* Values outside the lower limit.

reported in Table 3 the number of eyes and the relative percentage of normal and abnormal values detected in DOA group and separately in DOA-M and DOA-H groups.

Mean values and one standard deviation (SD) of mfERG N1-P1 RADs observed in controls, in DOA group, and separately in DOA-M and DOA-H groups and the relative statistical analysis (ANOVA Control versus DOA, DOA-M and DOA-H) are presented in Tables 4 and 5, respectively.

In Fig. 1 are presented examples of averaged mfERG recordings (ring and sector traces) obtained in a control, in a DOA-M (#4) and a DOA-H (#11) eye (Table 2).

Ring analysis

Considering the individual values, as presented in Table 3, the great percentage of all DOA eyes (63%) showed reduced N1-P1 RADs in ring 1, while in the other rings, we detected a percentage lower than 30% (ranging from the 11% of R5 to the 26% of R2) of abnormal N1-P1 RADs. When we considered separately the DOA eyes, in DOA-M group a percentage of abnormal N1-P1 RAD values >50% was detected in R1, R2, R3 and R4 rings, while in DOA-H group, it was observed only in R1; indeed, in the other rings, we observed a very small percentage (ranging from the 0% of R5 to the 8% of R2) of abnormal N1-P1 RADs (see Table 3).

On average, when compared to controls, the DOA group showed significantly reduced N1-P1 RAD mean values in ring 1, ring 2, ring 3 and ring 4 (Table 4). Dominant optic atrophy-M (DOA-M) eyes showed N1-P1 RAD mean values significantly reduced in all rings compared to controls,

Table 3. Number (Nr) and relative percentage (%) of normal [values of N1-P1 response amplitude density (RAD) – greater than the lower limit considered as the mean value −2 standard deviation of control subjects] or abnormal (values of N1-P1 RAD smaller than the lower limit considered as the mean value −2 standard deviation of control subjects) of multifocal electroretinogram (mfERG) responses observed in all patients affected by dominant optic atrophy (DOA), and, separately, in DOA patients with *OPA1* missense mutation (DOA-M) and in DOA patients with *OPA1* mutations causing haploinsufficiency (DOA-H).

mfERG N1-P1 RAD	DOA (35 eyes)		DOA-M (11 eyes)		DOA-H (24 eyes)	
	Normal	Abnormal	Normal	Abnormal	Normal	Abnormal
Sectors	Nr (%)	Nr (%)	Nr (%)	Nr (%)	Nr (%)	Nr (%)
R1	13 (37)	22 (63)	1 (9)	10 (91)	12 (50)	12 (50)
R2	26 (74)	9 (26)	4 (36)	7 (64)	22 (92)	2 (8)
R3	27 (77)	8 (23)	4 (36)	7 (64)	23 (96)	1 (4)
R4	29 (83)	6 (17)	5 (45)	6 (55)	24 (100)	0 (0)
R5	31 (89)	4 (11)	8 (73)	3 (27)	23 (96)	1 (4)
TS	33 (94)	2 (6)	9 (82)	2 (18)	24 (100)	0 (0)
TI	27 (77)	8 (23)	5 (45)	6 (55)	22 (92)	2 (8)
NS	23 (66)	12 (34)	6 (55)	5 (45)	17 (71)	7 (29)
NI	27 (77)	8 (23)	5 (45)	6 (55)	22 (92)	2 (8)
T	28 (80)	7 (20)	4 (36)	7 (64)	24 (100)	0 (0)
S	33 (94)	2 (6)	9 (82)	2 (18)	24 (100)	0 (0)
N	25 (71)	10 (29)	4 (36)	7 (64)	21 (87)	3 (13)
I	26 (74)	9 (26)	4 (36)	7 (64)	22 (92)	2 (8)

The mfERG responses have been evaluated in five annular retinal areas with different eccentricity from the fovea (ring 1: 0–5 degrees, R1; ring 2: 5–10 degrees, R2; ring 3: 10–15 degrees, R3; ring 4: 15–20 degrees, R4; and ring 5: 20–25 degrees, R5) and in eight sectors on the basis of the retinal topography: temporal–superior (TS), temporal–inferior (TI), nasal–superior (NS) and nasal–inferior (NI), temporal (T), superior (S), nasal (N) and inferior (I).

Table 4. Mean values and one standard deviation (SD) of multifocal electroretinogram (mfERG) N1-P1 response amplitude density (RAD) detected in control subjects (controls) and in patients affected by dominant optic atrophy (DOA).

mfERG	Controls (25 eyes)		DOA (35 eyes)		ANOVA DOA versus Controls	
Sector	Mean N1-P1 RAD (nV/degree^2)	SD	Mean N1-P1 RAD (nV/degree^2)	SD	F (1,59)	p
R1	166.27	35.31	105.91	47.15	29.21	**< 0.001**
R2	65.81	14.60	50.55	19.12	11.22	**0.001**
R3	36.22	8.63	28.59	9.14	10.65	**0.002**
R4	22.21	5.23	17.81	4.87	11.21	**0.001**
R5	16.57	2.87	15.42	4.55	1.24	0.270
TS	21.99	5.57	20.34	6.39	1.07	0.304
TI	26.71	5.24	22.37	6.61	7.43	**0.008**
NS	23.84	3.63	19.80	5.32	10.86	**0.002**
NI	26.28	5.93	22.22	6.44	6.67	0.012
T	26.18	6.53	22.44	8.84	3.22	0.078
S	20.53	4.60	18.48	4.74	2.81	0.099
N	26.4	4.95	20.76	6.55	13.16	**0.001**
I	25.8	6.05	21.78	7.46	4.94	0.030

The mfERG responses have been evaluated in five annular retinal areas with different eccentricity from the fovea (ring 1: 0–5 degrees, R1; ring 2: 5–10 degrees, R2; ring 3: 10–15 degrees, R3; ring 4: 15–20 degrees, R4; and ring 5: 20–25 degrees, R5) and in eight sectors on the basis of the retinal topography: temporal–superior (TS), temporal–inferior (TI), nasal–superior (NS) and nasal–inferior (NI), temporal (T), superior (S), nasal (N) and inferior (I).
ANOVA = one-way analysis of variance.
The bold values are statistically significant.

whereas DOA-H eyes showed a statistically significant reduction in N1-P1 RADs exclusively in ring 1 (Table 5).

Sector analysis 1

As specified before, values deriving from the most central retina (Ring 1, 0–5 degrees) were excluded from this analysis. Considering the individual mfERG responses, in DOA group we detected a small percentage (ranging from the 6% of TS to the 34% of NS sectors) of abnormal N1-P1 RAD values. In DOA-M group, the larger percentage (55%) of abnormal N1-P1 RAD values was observed in TI and NI sectors, while in TS and in NS sectors, only the 18% and 45% of eyes presented abnormal N1-P1 RAD values, respectively. In DOA-H group, the greater percentage (29%) of abnormal N1-P1 RAD values was observed only in NS sector; in fact in the other sectors, we detected that the greater percentage of eyes (ranging from the 71% of NS to the 100% of TS) showed normal N1-P1 RAD values (see Table 3).

On average, compared to controls, in DOA group, a significant reduction in N1-P1 RAD mean values (Table 4) was found in TI and NS sectors. In DOA-M group, N1-P1 RADs were significantly reduced when compared to those of controls in TI, NS and NI sectors. In DOA-H group, instead, we observed a significant reduction in N1-P1 RAD mean values only in the NS sector (Table 5).

Sector analysis 2

Considering the individual mfERG responses, in DOA group, we found a small percentage (ranging from the 6% of S to the 29% of N sectors) of abnormal N1-P1 RAD values. In DOA-M group, the larger percentage (64%) of abnormal N1-P1 RAD values was detected in T, N and I sectors, whereas in S sector, only the 18% of eyes presented abnormal N1-P1 RAD values. In DOA-H group, the greater percentage (13%) of abnormal N1-P1 RAD values was observed only in N sector; in fact in the other sectors, we observed that the greater percentage of eyes (ranging from the 92% of I sector to the 100% of T and S sectors) showed normal N1-P1 RAD values (see Table 3).

On average, when compared to controls, DOA group showed a significant reduction in N1-P1 RAD mean values only in the N sector (Table 4). In DOA-M eyes, N1-P1 RADs values were significantly reduced in the T, N and I sectors compared to controls. By contrast, no significant reduction in mean N1-P1 RADs was detected in

Table 5. Mean values and one standard deviation (SD) of multifocal electroretinogram (mfERG) N1-P1 response amplitude density (RAD) detected in control subjects (controls) and in patients affected by dominant optic atrophy with *OPA1* missense mutation (DOA-M) and with *OPA1* mutations causing haploinsufficiency (DOA-H).

mfERG Sector	Controls (25 eyes)		DOA-M (11 eyes)		ANOVA DOA-M versus controls		DOA-H (24 eyes)		ANOVA DOA-H versus controls	
	Mean N1-P1 RAD (nV/degree^2)	SD	Mean N1-P1 RAD (nV/degree^2)	SD	$F(1,35)$	p	Mean N1-P1 RAD (nV/degree^2)	SD	$F(1,48)$	p
R1	166.27	35.31	73.50	38.70	49.81	**< 0.001**	120.76	43.64	16.17	**< 0.001**
R2	65.81	14.60	38.23	13.88	28.04	**< 0.001**	56.20	18.74	4.03	0.050
R3	36.22	8.63	23.88	8.44	15.81	**0.001**	30.75	8.79	4.85	0.033
R4	22.21	5.23	15.99	4.29	11.94	**0.001**	18.64	4.98	5.99	0.018
R5	16.57	2.87	13.08	3.93	8.97	**0.005**	16.49	4.48	0.01	0.941
TS	21.99	5.57	17.66	6.30	4.25	0.047	21.57	6.17	0.06	0.805
TI	26.71	5.24	17.95	6.65	18.09	**< 0.001**	24.01	6.11	2.76	0.103
NS	23.84	3.63	19.02	6.11	8.76	**0.006**	20.16	5.01	8.78	**0.005**
NI	26.28	5.93	19.14	5.84	12.74	**0.001**	23.64	6.31	2.57	0.116

The mfERG responses have been evaluated in five annular retinal areas with different eccentricity from the fovea (ring 1: 0–5 degrees, R1; ring 2: 5–10 degrees, R2; ring 3: 10–15 degrees, R3; ring 4: 15–20 degrees, R4; and ring 5: 20–25 degrees, R5) and in eight sectors on the basis of the retinal topography: temporal–superior (TS), temporal–inferior (TI), nasal–superior (NS) and nasal–inferior (NI), temporal (T), superior (S), nasal (N) and inferior (I).
ANOVA = one-way analysis of variance.
The bold values are statistically significant.
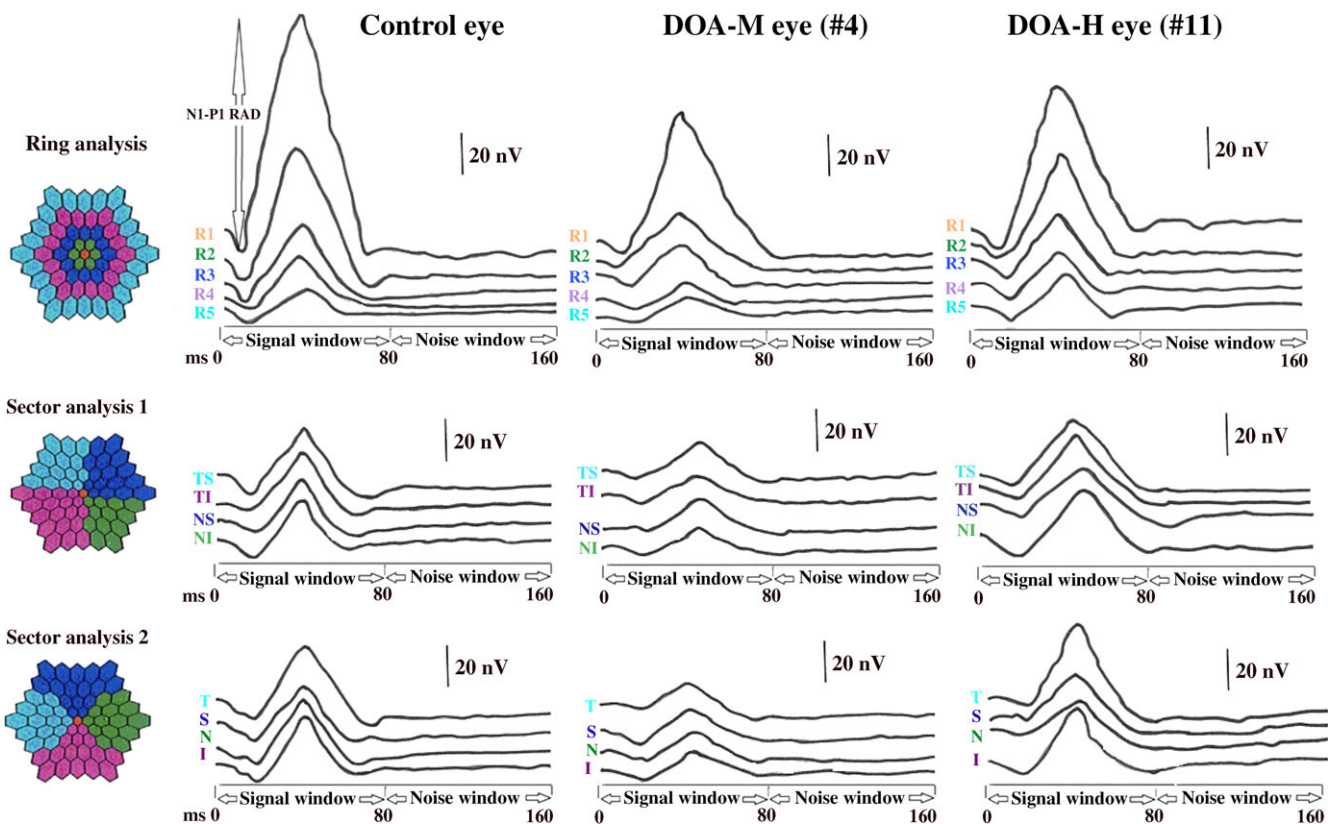
Fig. 1. Multifocal electroretinogram averaged recordings obtained in a control eye, in a patient with dominant optic atrophy (DOA) caused by OPA1 missense mutation (DOA-M#4 eye) and a patient with DOA caused by OPA1 mutation leading to haploinsufficiency (DOA-H#11 eye). Control, DOA-M#4 and DOA-H were right eyes. Ring analysis reports the averaged responses obtained from five concentric annular retinal regions (rings) centred on the fovea: from 0 to 5 degrees (ring 1, R1), from 5 to 10 degrees (ring 2, R2), from 10 to 15 degrees (ring 3, R3), from 15 to 20 degrees (ring 4, R4) and from 20 to 25 degrees (ring 5, R5). Sector analysis 1 reports the values of averaged response obtained from four areas on the basis of retinal topography: nasal–inferior (NI), nasal–superior (NS), temporal–inferior (TI) and temporal–superior (TS) sectors. The bioelectrical responses obtained from the central ring (R1, 0–5 central degrees) were excluded. Sector analysis 2 reports the values of averaged responses obtained from four areas on the basis of retinal topography: nasal (N), superior (S), inferior (I) and temporal (T) sectors. The bioelectrical responses obtained from the central ring (R1, 0–5 central degrees) were excluded. With respect to control eye, DOA-M#4 eye showed reduced N1-P1-response amplitude density (RADs) in R1, R2, R3, R4, TI, NS, NI, T, N and S sectors, while DOA-H#11 eye presented a reduction in N1-P1 RADs exclusively in R1 and N sectors.

DOA-H eyes as compared to controls (Table 5).

Discussion

This study evaluated the function of the retinal elements downstream of the photoreceptors but upstream from RGC axon hillocks (preganglionic) in patients affected by DOA to understand whether the retinal dysfunction may manifest differently in the presence of *OPA1* missense mutations or *OPA1* mutations causing haploinsufficiency. For this reason, we evaluated the retinal bioelectrical responses from different retinal areas (rings and sectors), based on the three possible presentations of the retinal topography to selectively detect the areas that might present the prevalent preganglionic impairment in this hereditary optic neuropathy.

We studied selectively the first-order kernel of mfERG responses, generated by the outer and, in minor part, by the inner retinal layers (photoreceptors and bipolar cells) (Hood et al. 2012). Previous studies suggested that an abnormal mfERG waveform provides strong evidence for preganglionic (i.e. amacrine cells, bipolar cells and GC dendrites) dysfunction (Hood 2000; Miyata et al. 2007; Reis et al. 2013). Therefore, in DOA patients, the abnormal RADs of the first-order kernel of mfERG responses may be ascribed to a dysfunction of retinal preganglionic elements.

Using the standard ring analysis, we were able to recognize that DOA eyes behaved very differently as compared to control eyes. In fact, we described a reduced preganglionic central retinal response with a relative sparing of the most peripheral ring (R5).

By means of the sector analyses 1 and 2, we wanted to exclude from the data set the RAD values recorded from ring 1 (0–5 degrees), therefore eliminating the contribution from the most central retina. We found that all DOA eyes showed a prevalent dysfunction of the TI and the NS sectors and overall of the N sector. This result confirmed the preferential involvement of the nasal sectors corresponding to the anatomical distribution of the papillomacular bundle, as previous detected by Optical coherence tomography (OCT) in DOA patients (Barboni et al. 2011).

Moreover, when we separated our DOA eyes in two subgroups, based on the genetic mutation type, we found

that, while DOA-H eyes had a dysfunction selectively localized at the 0–5 degrees of eccentricity and in the NS sector, DOA-M eyes presented a widespread preganglionic dysfunction sparing only the TS and the S sectors.

Previous studies in *OPA1* animal models showed normal ERG responses (Alavi et al. 2007; Heiduschka et al. 2010) and a significant reduction in the photopic negative response (PhNR) amplitude (Barnard et al. 2011), suggesting normal photoreceptor function, with an impairment of the inner nuclear and plexiform layers, including the amacrine cells. In fact, PhNR probably reflects activity of RGCs and their axons with contributions from amacrine cells and possible involvement of associated glial cells/astrocytes of the retina (Viswanathan et al. 1999; Rangaswamy et al. 2007).

There have been only a few studies that attempted to evaluate preganglionic function in humans affected by DOA: no alterations were found in flash ERG responses by Miyata et al. 2007; who described normal photoreceptor function. Only oscillatory potentials (OP) were found reduced. The cellular origin of OPs is not yet clear, but they probably originate from feedback neural pathways in the inner retina, especially around the inner plexiform layer, with large contributions from amacrine cells, although RGCs and bipolar cells may also contribute to parts of the OPs (Heynen et al. 1985; Rangaswamy et al. 2006). Moreover, also PhNR was found reduced in DOA patients (Miyata et al. 2007; Morny et al. 2015).

Conflicting results were found in previous studies using mfERG. No alterations were found in DOA patients by Granse et al. (2003); however, they analysed only seven members from the same family carrying an *OPA1* mutation causing haploinsufficiency. Their results are quite consistent with our own results showing only minor mfERG alterations in DOA-H patients. Our DOA-H patients, in fact, showed reduced RADs only in the central ring. We are confident that our results were not affected by fixation losses as we did select the cohort of patients without central scotoma and with good fixation. Also, our findings in DOA-H patients were not affected by the different amount of examined eyes in the two groups, being the DOA-H group the largest.

Similarly to our results, Reis et al. (2013) showed mfERG alteration in DOA as detected by P1 wave amplitudes reduction. Moreover, mfERG responses were correlated with retinal thickness and visual acuity. The evidence of preganglion impairment could be explained by the fact that *OPA1* is expressed not only in the RGCs and in their axons, but also, to a lesser extent, in the inner plexiform, inner nuclear and outer plexiform layers (Aijaz et al. 2004; Bertholet et al. 2013; More likely, most of the cellular damage occurs to the RGCs laden with *OPA1*. However, these RGCs go through stages of involution prior to degeneration. Early impairment may begin with the distal GC dendrites, as has been shown by Votruba et al. (1998), in their animal model (Alexander et al. 2000). There is clear evidence for the important role played by *OPA1* in maintaining the postsynaptic dendritic integrity of RGCs. Possibly, the preganglionic electrophysiological defect is due to the failure of bipolar and amacrine cell terminals to produce a robust signal on GCs.

When DOA patients were selectively examined on the basis of the specific *OPA1* mutation, we observed that DOA-M showed more severe impairment than DOA-H. In the latter group, the mfERG reduction was minimal. In agreement with the already described phenotype–genotype correlation in DOA patients (Barboni et al. 2014), the present results suggest that *OPA1* missense mutations induce a greater vulnerability of the preganglionic elements.

The present study has some limitations: first of all, we used a small simple size and there was disproportionate distribution in DOA groups, but the haploinsufficiency is the most common disease mechanism (Liskova et al. 2017) and our sample confirms it. However, DOA is a rare disease, and the *OPA1* missense mutations are less frequently found. Second, we analysed both patients' eyes, and this approach is problematic from a statistical point of view. Again, the rarity of DOA patients justifies the inclusion of both eyes.

In conclusion, we recognized a preganglionic impairment in DOA. A clear genotype–phenotype association emerged stratifying mfERG measures by OPA1 mutation type, with the most severe being missense mutations. Thus,

mfERG can be useful to functionally differentiate DOA patients based on *OPA1* mutation, guiding clinical management of patients. In addition, the results provided by mfERG recordings may improve the possibility to understand the multifactorial retinal neurophysio-pathological mechanisms that induce a visual impairment in patients with OPA1 mutation.

References

Aijaz S, Erskine L, Jeffery G, Bhattacharya SS & Votruba M (2004): Developmental expression profile of the optic atrophy gene product: OPA1 is not localized exclusively in the mammalian retinal ganglion cell layer. Invest Ophthalmol Vis Sci **45**: 1667–1673.

Alavi MV, Bette S, Schimpf S et al. (2007): A splice site mutation in the murine Opa1 gene features pathology of autosomal dominant optic atrophy. Brain **130**: 1029–1042.

Alexander C, Votruba M, Pesch UE et al. (2000): OPA1, encoding a dynamin-related GTPase, is mutated in autosomal dominant optic atrophy linked to chromosome 3q28. Nat Genet **26**: 211–215.

Barboni P, Savini G, Cascavilla M et al. (2014): Early macular retinal ganglion cell loss in dominant optic atrophy: genotype-phenotype correlation. Am J Ophthalmol **158**: 628–636.

Barboni P, Savini G, Parisi V et al. (2011): Retinal nerve fiber layer thickness in dominant optic atrophy measurements by optical coherence tomography and correlation with age. Ophthalmology **118**: 2076–2080.

Barnard AR, Charbel Issa P, Perganta G, Williams PA, Davies VJ, Sejaran S, Votruba M & MacLaren RE (2011): Specific deficits in visual electrophysiology in a mouse model of dominant optic atrophy. Exp Eye Res **93**: 771–777.

Bearse MA Jr & Sutter EE (1996): Imaging localized retinal dysfunction with the multifocal electroretinogram. J Opt Soc Am A Opt Image Sci Vis **13**: 634–640.

Bertholet AM, Millet AM, Guillermin O, Daloyau M, Davezac N, Miquel MC & Belenguer P (2013): OPA1 loss of function affects in vitro neuronal maturation. Brain **136**: 1518–1533.

Chan HH (2005): Detection of glaucomatous damage using multifocal ERG. Clin Exp Optom **88**: 410–414.

Chan HH & Brown B (2000): Pilot study of the multifocal electroretinogram in ocular hypertension. Br J Ophthalmol **84**: 1147–1153.

Chan HH, Ng YF & Chu PH (2011): Applications of the multifocal electroretinogram in the detection of glaucoma. Clin Exp Optom **94**: 247–258.

Delettre C, Lenaers G, Griffoin JM et al. (2000): Nuclear gene OPA1, encoding a mitochondrial dynamin-related protein, is mutated in dominant optic atrophy. Nat Genet **26**: 207–210.

Granse L, Bergstrand I, Thiselton D, Ponjavic V, Heijl A, Votruba M & Andréasson S (2003): Electrophysiology and ocular blood flow in a family with dominant optic nerve atrophy and a mutation in the OPA1 gene. Ophthalmic Genet **24**: 233–245.

Heiduschka P, Schnichels S, Fuhrmann N, Hofmeister S, Schraermeyer U, Wissinger B & Alavi MV (2010): Electrophysiological and histologic assessment of retinal ganglion cell fate in a mouse model for OPA1-associated autosomal dominant optic atrophy. Invest Ophthalmol Vis Sci **51**: 1424–1431.

Heynen H, Wachtmeister L & van Norren D (1985): Origin of the oscillatory potentials in the primate retina. Vision Res **25**: 1365–1373.

Holder GE, Votruba M, Carter AC, Bhattacharya SS, Fitzke FW & Moore AT (1998-1999): Electrophysiological findings in dominant optic atrophy (DOA) linking to the OPA1 locus on chromosome 3q 28-qter. Doc Ophthalmol **95**: 217–228.

Hood DC (2000): Assessing retinal function with the multifocal technique. Prog Retin Eye Res **19**: 607–646.

Hood DC, Odel JG, Chen CS & Winn BJ (2003): The multifocal electroretinogram. J Neuroophthalmol **23**: 225–235.

Hood DC, Bach M, Brigell M et al. (2012): ISCEV standard for clinical multifocal electroretinography (mfERG) (2011 edition). Doc Ophthalmol **124**: 1–13.

Lenaers G, Hamel C, Delettre C, Amati-Bonneau P, Procaccio V, Bonneau D, Reynier P & Milea D (2012): Dominant optic atrophy. Orphanet J Rare Dis **7**: 46.

Liskova P, Tesarova M, Dudakova L, Svecova S, Kolarova H, Honzik T, Seto S & Votruba M (2017): OPA1 analysis in an international series of probands with bilateral optic atrophy. Acta Ophthalmol **95**: 363–369.

Miyata K, Nakamura M, Kondo M, Lin J, Ueno S, Miyake Y & Terasaki H (2007): Reduction of oscillatory potentials and photopic negative response in patients with autosomal dominant optic atrophy with OPA1 mutations. Invest Ophthalmol Vis Sci **48**: 820–824.

Morny EK, Margrain TH, Binns AM & Votruba M (2015): Electrophysiological ON and OFF responses in autosomal dominant optic atrophy. Invest Ophthalmol Vis Sci **56**: 7629–7637.

Parisi V, Ziccardi L, Stifano G, Montrone L, Gallinaro G & Falsini B (2010): Impact of regional retinal responses on cortical visually evoked responses: multifocal ERGs and VEPs in the retinitis pigmentosa model. Clin Neurophysiol **121**: 380–385.

Parisi V, Ziccardi L, Centofanti M, Tanga L, Gallinaro G, Falsini B & Bucci MG (2012): Macular function in eyes with open-angle glaucoma evaluated by multifocal electroretinogram. Invest Ophthalmol Vis Sci **53**: 6973–6980.

Rangaswamy NV, Zhou W, Harwerth RS & Frishman LJ (2006): Effect of experimental glaucoma in primates on oscillatory potentials of the slow-sequence mfERG. Invest Ophthalmol Vis Sci **47**: 753–767.

Rangaswamy NV, Shirato S, Kaneko M, Digby BI, Robson JG & Frishman LJ (2007): Effects of spectral characteristics of ganzfeld stimuli on the photopic negative response (PhNR) of the ERG. Invest Ophthalmol Vis Sci **48**: 4818–4828.

Reis A, Mateus C, Viegas T, Florijn R, Bergen A, Silva E & Castelo-Branco M (2013): Physiological evidence for impairment in autosomal dominant optic atrophy at the pre-ganglion level. Graefes Arch Clin Exp Ophthalmol **251**: 221–234.

Viswanathan S, Frishman LJ, Robson JG, Harwerth RS & Smith EL III (1999): The photopic negative response of the macaque electroretinogram: reduction by experimental glaucoma. Invest Ophthalmol Vis Sci **40**: 1124–1136.

Votruba M, Fitzke FW, Holder GE, Carter A, Bhattacharya SS & Moore AT (1998): Clinical features in affected individuals from 21 pedigrees with dominant optic atrophy. Arch Ophthalmol **116**: 351–358.

Wilsey LJ & Fortune B (2016): Electroretinography in glaucoma diagnosis. Curr Opin Ophthalmol **27**: 118–124.

Yu-Wai-Man P, Griffiths PG & Chinnery PF (2011): Mitochondrial optic neuropathies – disease mechanisms and therapeutic strategies. Prog Retin Eye Res **30**: 81–114.

Correspondence
Piero Barboni
Scientific Institute San Raffaele Via Olgettina 60, 20123 Milan
Italy
Tel/Fax: +390226433589
Email: p.barboni@studiodazeglio.it